

Precursor States in the Adsorption of Sb_4 on Si(001)

Y. W. Mo

IBM T.J. Watson Research Center, Yorktown Heights, New York 10598

(Received 20 July 1992)

The surprising complexity of the reaction path of the dissociation of Sb_4 on Si(001) is revealed by scanning tunneling microscopy (STM). Four distinct types of precursors are identified, which can be converted to the final state of two-dimer clusters through thermal annealing, or through a novel STM-tip-induced conversion. An effective energy barrier of 0.5 ± 0.1 eV and an effective prefactor of $\sim 10^3$ Hz are measured for the thermal conversion of precursors to the final state. The results indicate that popular models assuming only one precursor state may fail for many semiconductor systems.

PACS numbers: 61.16.Di, 68.10.Jy

The kinetics of adsorption of atoms or molecules on solid surfaces is an important subject in surface science. In particular, the existence and the role of precursors in dissociative adsorption are of great interest. The concept of a precursor state was first introduced by Langmuir in 1929 [1], and since then there have been many studies of precursor states in the adsorption of molecules on metal [2] and, to a lesser extent, semiconductor surfaces [3,4]. However, most of the evidence for the existence of precursors is rather indirect, and quantitative information on the stabilities of precursors is primarily derived from measuring adsorption and desorption rates. Direct observation of precursors and quantitative measurements of their conversion kinetics using microscopic methods are desirable for understanding the details of the interaction of molecules with solid surfaces.

The interaction of dopant molecules with semiconductor surfaces affects their incorporation in semiconductor films grown by vapor phase deposition. There is much interest in the role of molecular precursor states in determining the incorporation efficiency of common dopants for silicon such as Sb, As, P, and B, because they are often deposited in molecular form. Most studies so far, however, have been based on macroscopic methods and the assumption of a single precursor state [3,4].

The growth of Sb on Si(001) has attracted much attention because of its applications in making delta-doping structures [5] and in the surfactant-mediated growth of Ge on Si(001) [6]. There have been studies on the adsorption-desorption parameters and on the final structures of the Sb overlayer at near full monolayer (ML) coverage [7-10]. In particular, scanning tunneling microscopy (STM) and extended x-ray-absorption fine structure studies have concluded that the Sb overlayer deposited at elevated temperatures on Si(001) forms a dimer reconstruction, with dimer bonds perpendicular to those of the Si(001) substrate, but the kinetic path to reach this structure via precursor states has not been investigated [9].

In this Letter, we report STM studies of the adsorption kinetics of Sb_4 on Si(001), revealing the complexity of the reaction path which involves four distinct types of

precursor states. The precursors are metastable at room temperature but can be converted to the final state by thermal annealing at as low as 327 K. We have also discovered that the conversion can be induced by a high bias, e.g., 3 V, on the STM tip. This process enables us to identify without ambiguity the precursor clusters as being made of four Sb atoms. These unique features of this system provide a rare opportunity for studying and controlling, step by step, the reaction path of a molecule with a semiconductor surface. The stabilities of the precursors are studied quantitatively by counting, in the STM images, the population distribution of cluster types as a function of thermal treatment. These results indicate that popularly employed models based on the assumption of only one precursor state may be too simple for many systems.

The experiments were carried out in an ultrahigh-vacuum chamber equipped with STM, mass spectrometer, and Sb source. The base pressure of the system is $\sim 4 \times 10^{-11}$ Torr. It is well known that when heated in the bulk form at temperatures below ~ 800 K, Sb evaporates nearly exclusively as Sb_4 [4,11]. Based on the mass spectrometry studies of Sb desorption from Si(001) by Barnett, Winters, and Greene [4], we have built an Sb source that works by evaporating Sb_4 from a quartz tube toward another Si(001) wafer which serves as a "Si mirror" to bounce Sb back to the sample [10]. By controlling the Si mirror temperature, we can selectively deposit either Sb_4 or Sb_1 . Direct evaporation of Sb_4 from the quartz tube onto the sample is also employed and it yields the same results as those when Sb_4 is bounced back to the sample from the Si mirror kept at 673 K. The substrate is cleaned by heating briefly to ~ 1525 K. The deposition rate is determined by counting Sb atoms in STM images; a monolayer is defined as one Sb atom for each Si atom in the top layer of Si(001). Sample temperature is measured by a W-5%Re/W-26%Re thermocouple and its uncertainty is estimated to be ± 10 K.

Upon deposition at room temperature of 0.02 ML of Sb_4 on Si(001), the final state as well as the precursor clusters are observed, as shown in Fig. 1. Each of the final-state clusters is made of two dimers with the dimer

bonds perpendicular to those of the substrate (labeled *E* in Fig. 1) [12]. There are several variations in the relative positions of the two dimers in each final-state cluster (not all shown in Fig. 1), but all of them are classified as the final state. There are four distinct types of precursor clusters. One of them appears as a tiny ball without any visible internal features, and appears much higher than the other types of clusters (*A*). We refer to this type as the "ball" cluster. Another type consists of a pair of "dimers" with their dimer bonds parallel to those of the substrate (*B*). These are denoted as "rotated dimers." Some clusters consist of one normal dimer and one rotated dimer. These are still counted as rotated dimers in the following distribution measurements, instead of a separate type. The remaining types both have two pronounced peaks with two weaker peaks in between. We call the one with the long axis parallel to the substrate dimer rows "dumbbells" (*C*), and the one with the long

axis perpendicular to the substrate dimer rows "rotated dumbbells" (*D*). Four dumbbells and one rotated dumbbell are shown in Fig. 1(a). A different image obtained with a lower bias voltage is shown in Fig. 1(b), revealing more features in the clusters. Filled-state images such as those shown in Fig. 1 have better resolution than the empty-state images which typically yield a much smaller apparent height of the Sb clusters. This behavior

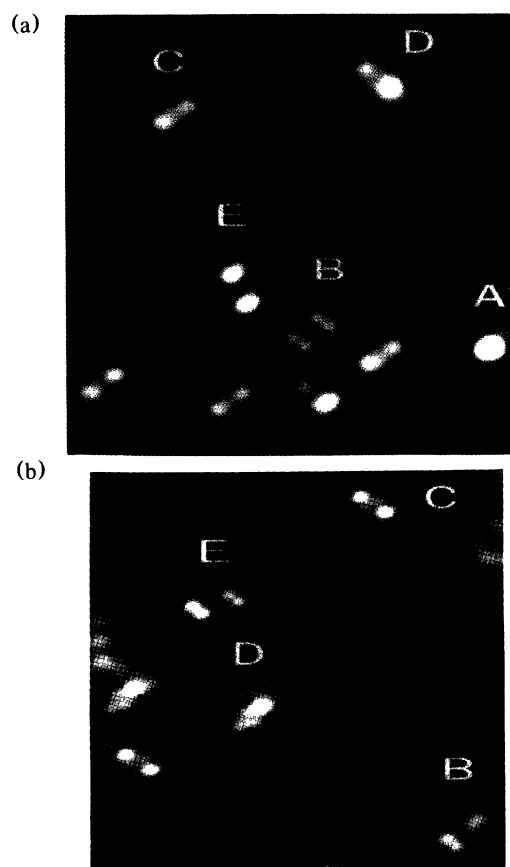


FIG. 1. STM images of Sb clusters on Si(001) deposited at room temperature. (a) Five types of clusters: one "ball" (*A*), two "rotated dimers" (*B*), four "dumbbells" (*C*), one "rotated dumbbell" (*D*), and one final state of the two-dimer cluster (*E*). Image size: $100 \times 100 \text{ \AA}$. Tip bias: +1.0 V. Tunneling current: 0.2 nA. (b) Higher-resolution imaging of one case of rotated dimers (*B*), two dumbbells (*C*), two rotated dumbbells (*D*), and one final state (*E*). At this bias of +0.7 V, more features are visible in the clusters. Image size: $90 \times 90 \text{ \AA}$.

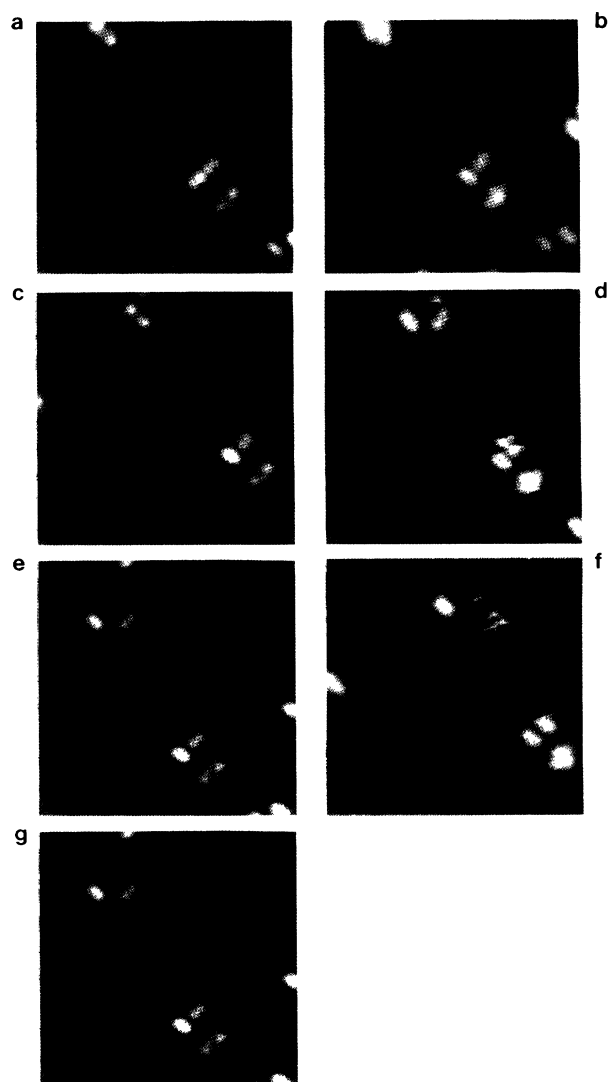


FIG. 2. Examples of STM-tip-induced "switching" of precursors into the final state. The images on the left are taken with a tip bias of +1.0 V which causes no structural change. The images on the right are taken at +3.0 V and each scan results in some changes in the precursor clusters. All scans are taken with a constant current of 0.4 nA. The last scan (g) shows that all precursors have been converted to the final state. Comparison between (c) and (e) also shows that the buckling phase of several substrate dimers near a defect is altered by the high bias scan (d), but the statistics are not yet sufficient to check the consistency of this phenomenon. The time sequence of the scans is (a) \rightarrow (g).

is opposite to that of the group-III elements on Si(001) [13]. Atomic models are not presented here for the precursors, because with STM alone we cannot unequivocally determine their detailed structures, although the STM images provide some hints for their likely configurations.

At room temperature, and scanning with low bias voltages, e.g., 1.0 V, the precursors are stable for more than one day. Upon thermal annealing, all precursors can be converted to the final state. Furthermore, we discover that the conversion of each type of precursor to the final state can be induced by scanning at higher bias voltages, e.g., 3.0 V, both polarities [14]. Figure 2 is a series of consecutive "observing" (+1.0 V tip bias) and "switching" (+3.0 V tip bias) scans, illustrating the tip-induced conversion of three types of precursors to the final state. Because of space limitations, examples of switching the ball precursors are not shown. The tip-induced conversion enables us to establish a one-to-one correspondence between each type of precursor cluster and the final state, and it also shows that care must be taken when studying precursors with probe beams of enough energy to cause their conversion.

To check that the formation of exclusively four-atom clusters is due to the deposition of Sb_4 , we deposit Sb_1 on Si(001) at room temperature by keeping the Si mirror of the Sb source at 1173 K. This results in a random distribution of island sizes with the smallest islands observed being single dimer, indicating that single Sb atoms are mobile at room temperature, similar to that of Si/Si(001) [15]. None of the precursors described above is observed.

Having confirmed the identities of the observed clusters, we study quantitatively the thermal stability of the precursors by measuring the population of each type of cluster after anneals at different temperatures. In Table I, we list the fractional population of each type of cluster after consecutive anneals at three temperatures for 20 min each, together with the starting distribution of clusters deposited at room temperature. The error estimate includes the shot noise and the uncertainty in characterizing certain clusters that happen to be near surface defects. Because of the low Sb coverage, the change for two Sb_4 molecules to land at the same site is very low and hence does not affect the counting. The total number of each cluster type counted is typically more than several

hundred. To assure that there is no measurable desorption of the precursors during annealing, the total coverage of all Sb clusters after each anneal is measured using the counting results. The coverage remains constant, 0.02 ML, within the uncertainty in the counting and accuracy of scan areas. This is also a good indication of the internal consistency of the counting.

Several important points are found in Table I. First, it can be seen that the population distribution among the five cluster types deposited at room temperature is rather uniform, without a dominant species. Currently we do not know what determines the outcome of the landing of an individual incoming Sb_4 . We speculate that the exact impact point and/or the molecular orientation of Sb_4 at the moment of landing may be relevant. Second, it is clear that the balls are the least stable precursor, and at least some of them convert to other types of precursors before reaching the final state. This can be seen from the rapid decay in the ball population and the accompanying temporary rise in the populations of the rotated dimers and the rotated dumbbells after annealing at 327 K. These same behaviors are also observed in the STM-tip-induced conversion [16].

Since there are four types of precursors and the detailed path of the conversion of each type to the final state is not fully understood, we cannot readily measure the kinetic parameters for each step in the transition. Instead, we attempt to obtain an effective characterization of the whole conversion process by measuring the decay rate of the sum of all the precursors. Although this approach does not yield much physical insight for the microscopic mechanism of the transition, it nevertheless provides an estimate of the stability of the precursors.

In analogy to radioactive decay processes, we can write the population decay of the sum of all precursors, N , as

$$N = N_0 e^{-\lambda t}, \quad (1)$$

where λ is the effective decay rate of the total precursor population. λ is assumed to be of the form $\lambda = \lambda_0 e^{-E/kT}$, where E is the effective activation energy for the thermal conversion [2]. λ is obtained at several temperatures by measuring the changes in the sum of all precursors after each anneal. The results, as shown in Fig. 3, yield an effective activation energy of 0.5 ± 0.1 eV and an

TABLE I. The fractional population distribution of Sb cluster after consecutive anneals at three temperatures, together with the distribution after deposition at room temperature (300 K).

	As Deposited at 300 K	Annealed at 327 K	Annealed at 352 K	Annealed at 410 K
Final state	0.27 ± 0.02	0.32 ± 0.02	0.45 ± 0.03	0.91 ± 0.04
Rotated dimers	0.15 ± 0.01	0.17 ± 0.01	0.20 ± 0.01	0.010 ± 0.005
Ball	0.21 ± 0.01	0.06 ± 0.01	0.010 ± 0.006	0.004 ± 0.002
Dumbbell	0.20 ± 0.01	0.18 ± 0.01	0.18 ± 0.01	0.06 ± 0.01
Rotated dumbbell	0.17 ± 0.01	0.27 ± 0.01	0.16 ± 0.01	0.010 ± 0.005

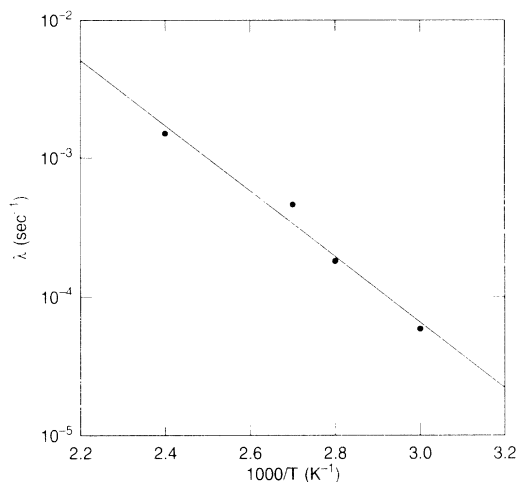


FIG. 3. The conversion rate of precursors to the final state, as a function of temperature. The slope yields an effective activation energy of 0.5 ± 0.1 eV.

effective prefactor of $\sim 10^3$ Hz. The low prefactor explains the fact that the precursors are metastable at room temperature despite the low activation energy for conversion. Again, these parameters are only effective characterizations of the whole conversion process which involves many microscopic steps, and they should not be compared to those in a well-defined microscopic transition. Work is under way to study separately the specific transitions between all states.

In summary, we have studied, using STM, the surprisingly complicated adsorption kinetics of Sb_4 on $\text{Si}(001)$ which involves four distinct types of precursors. An STM-tip-induced conversion process enables us to confirm unambiguously the identities of these precursors. An effective activation energy of 0.5 ± 0.1 eV and an effective prefactor of $\sim 10^3$ Hz are measured for the thermal conversion of the precursors to the final state. The STM methodology used here provides a straightforward method for studying such complicated systems with many coexisting precursors, which can be extremely difficult to identify with other methods. The complex nature of this system indicates that popular models based on the assumption of single precursor state may be too sim-

ple for many semiconductor systems [3,4].

The author would like to thank J. Demuth, R. Walkup, and B. Swartzentruber for valuable discussions, and M. Copel for assistance in making figures.

-
- [1] I. Langmuir, *Chem. Rev.* **6**, 451 (1929).
 - [2] For a review, see W. H. Weinberg, in *Kinetics of Interface Reactions*, edited by M. Grunze and H. Kreuzer (Springer-Verlag, Berlin, Heidelberg, 1987), and references therein.
 - [3] C. T. Foxon and B. A. Joyce, *Surf. Sci.* **50**, 434 (1975).
 - [4] S. A. Barnett, H. F. Winters, and J. E. Greene, *Surf. Sci.* **165**, 303 (1986).
 - [5] J. C. Bean, *Appl. Phys. Lett.* **33**, 654 (1978).
 - [6] M. Copel, M. C. Reuter, E. Kaxiras, and R. M. Tromp, *Phys. Rev. Lett.* **63**, 632 (1989).
 - [7] R. A. Metzger and F. G. Allen, *Surf. Sci.* **137**, 397 (1984).
 - [8] D. H. Rich, G. E. Franklin, F. M. Leibsle, T. Miller, and T.-C. Chiang, *Phys. Rev. B* **40**, 11804 (1989).
 - [9] M. Richter, J. C. Woicik, J. Nogami, P. Pianetta, K. E. Miyano, A. A. Baski, T. Kendelewicz, C. E. Bouldin, W. E. Spicer, C. F. Quate, and I. Lindau, *Phys. Rev. Lett.* **65**, 3417 (1990).
 - [10] W. F. J. Slijkerman, P. M. Zagwijn, and J. F. van der Veen, *Surf. Sci.* **262**, 25 (1992).
 - [11] R. Hultgren, R. L. Orr, P. D. Anderson, and K. K. Kelly, *Selected Values of Thermodynamic Properties of Elements* (Wiley, New York, 1973), p. 448.
 - [12] H. B. Elswijk and E. J. van Loenen, *Ultramicroscopy* **42-44**, 884 (1992).
 - [13] A. A. Baski, J. Nogami, and C. F. Quate, *J. Vac. Sci. Technol. A* **9**, 1946 (1991).
 - [14] STM-tip-induced changes in the adsorbates on solid surfaces have been reported on other systems, see, e.g., In-Whan Lyo and Ph. Avouris, *J. Chem. Phys.* **93**, 4479 (1990); D. M. Eigler and E. K. Schweizer, *Nature (London)* **344**, 524 (1990); L. J. Whitman, J. A. Stroscio, R. A. Dragoset, and R. J. Celotta, *Science* **251**, 1206 (1991); G. Dujardin, R. E. Walkup, and Ph. Avouris, *Science* **255**, 1232 (1992).
 - [15] Y. W. Mo, R. Kariotis, B. S. Swartzentruber, M. B. Webb, and M. G. Lagally, *J. Vac. Sci. Technol. A* **8**, 201 (1990).
 - [16] Y. W. Mo (to be published).

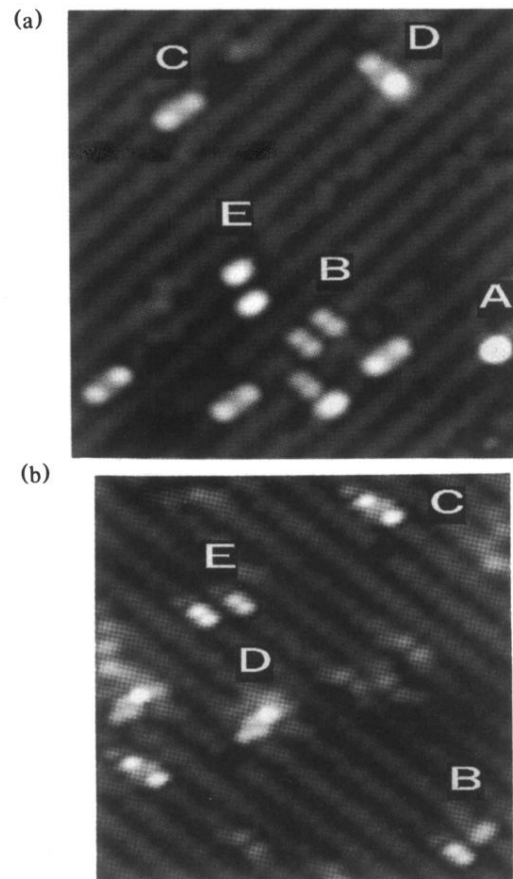


FIG. 1. STM images of Sb clusters on Si(001) deposited at room temperature. (a) Five types of clusters: one “ball” (*A*), two “rotated dimers” (*B*), four “dumbbells” (*C*), one “rotated dumbbell” (*D*), and one final state of the two-dimer cluster (*E*). Image size: $100 \times 100 \text{ \AA}$. Tip bias: +1.0 V. Tunneling current: 0.2 nA. (b) Higher-resolution imaging of one case of rotated dimers (*B*), two dumbbells (*C*), two rotated dumbbells (*D*), and one final state (*E*). At this bias of +0.7 V, more features are visible in the clusters. Image size: $90 \times 90 \text{ \AA}$.

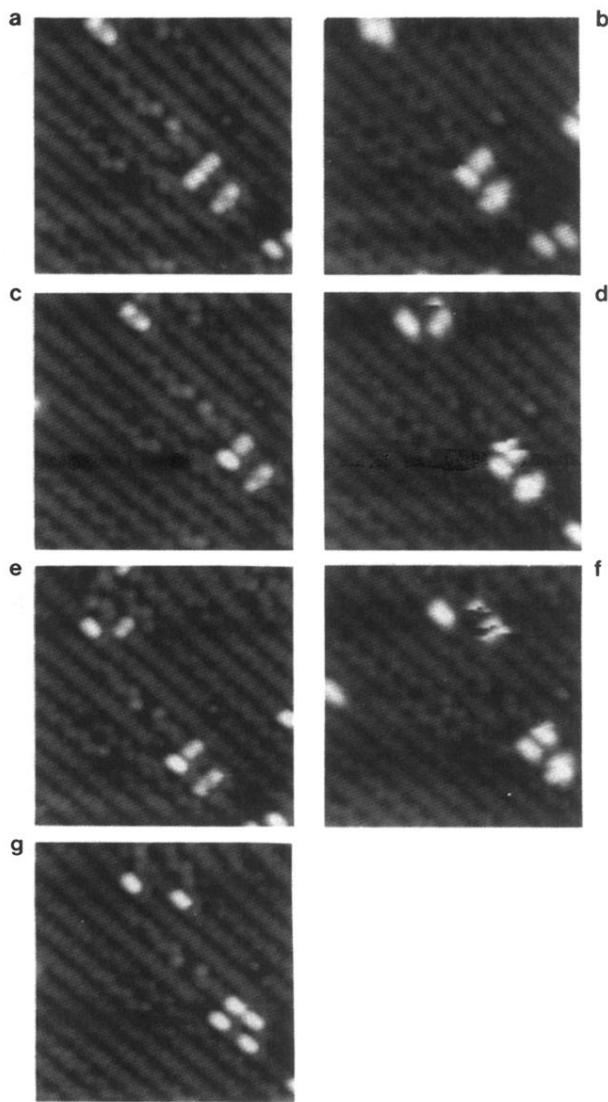


FIG. 2. Examples of STM-tip-induced “switching” of precursors into the final state. The images on the left are taken with a tip bias of +1.0 V which causes no structural change. The images on the right are taken at +3.0 V and each scan results in some changes in the precursor clusters. All scans are taken with a constant current of 0.4 nA. The last scan (g) shows that all precursors have been converted to the final state. Comparison between (c) and (e) also shows that the buckling phase of several substrate dimers near a defect is altered by the high bias scan (d), but the statistics are not yet sufficient to check the consistency of this phenomenon. The time sequence of the scans is (a) \rightarrow (g).